Renner-Teller and spin-orbit vibronic coupling effects in linear triatomic molecules with a half-filled π shell

Ilias Sioutis,[1,a)] Sabyashachi Mishra,[2] Leonid V. Poluyanov,[3] and Wolfgang Domcke[1,b)]
[1]*Department of Chemistry, Technical University of Munich, D-85747 Garching, Germany*
[2]*Department of Chemistry, University of Basel, CH-4056 Basel, Switzerland*
[3]*Institute of Chemical Physics, Academy of Sciences, Chernogolovka, Moscow 14232, Russia*

(Received 18 December 2007; accepted 14 January 2008; published online 31 March 2008)

The vibronic and spin-orbit-induced interactions among the $^3\Sigma^-$, $^1\Delta$, and $^1\Sigma^+$ electronic states arising from a half-filled π orbital of a linear triatomic molecule are considered, employing the microscopic (Breit-Pauli) spin-orbit coupling operator. The 6×6 Hamiltonian matrix is derived in a diabatic spin-orbital electronic basis set, including terms up to fourth order in the expansion of the molecular Hamiltonian in the bending normal coordinate about the linear geometry. The symmetry properties of the Hamiltonian are analyzed. Aside from the nonrelativistic fourth-order Renner-Teller vibronic coupling within the $^1\Delta$ state and the second-order nonrelativistic vibronic coupling between the $^1\Sigma^+$ and $^1\Delta$ states, there exist zeroth-order, first-order, as well as third-order vibronic coupling terms of spin-orbit origin. The latter are absent when the phenomenological expression for the spin-orbit coupling operator is used instead of the microscopic form. The effects of the nonrelativistic and spin-orbit-induced vibronic coupling mechanisms on the $^3\Sigma^-$, $^1\Delta$, and $^1\Sigma^+$ adiabatic potential energy surfaces as well as on the spin-vibronic energy levels are discussed for selected parameter values. © *2008 American Institute of Physics*. [DOI: 10.1063/1.2840356]

I. INTRODUCTION

It has previously been shown that the inclusion of the microscopic Breit-Pauli spin-orbit (SO) operator in the molecular Hamiltonian of linear triatomic molecules gives rise to novel vibronic coupling terms for $^2\Pi$ degenerate electronic states.[1,2] The vibronic coupling terms arising from the two-electron Breit-Pauli operator have also been discussed for $^3\Pi$ electronic states of linear triatomic molecules.[3] It has been found that in addition to the nonrelativistic Renner-Teller coupling term, which is of second order in the bending amplitude (in $^2\Pi$ electronic states), there exist SO-induced vibronic coupling terms which are of first order in the bending amplitude.[1–3] In the present work, we proceed one step further and develop a model for the description of the combined effects of Renner-Teller and SO coupling of linear triatomic molecules with a half-filled π shell. This approach employs the microscopic Breit-Pauli SO operator for two active electrons. It may be applied for a wide range of linear or quasilinear molecules ranging from simple carbenes to heavier molecular systems.

Carbenes play an important role in combustion,[4,5] stratospheric[6] and interstellar chemistry,[7,8] as well as in organic and organometallic reactions[9–12] and processes that involve thermal degradation of small organic molecules.[13] The prototypical carbene methylene (CH_2) has been a favorite target of spectroscopists[14–16] and theoreticians[17–20] for nearly half a century, due to its fundamental role as a radical intermediate species in gas-phase chemical reactions.[21] Moreover, it is sufficiently small to serve as a benchmark molecular system for the development of *ab initio* electronic-structure methods. From an electronic-structure point of view, CH_2 is a linear molecule with a half-filled π shell, since two of its valence electrons occupy a degenerate π orbital. This electronic configuration gives rise to the $^3\Sigma_g^-$, $^1\Delta_g$ and $^1\Sigma_g^+$ electronic states, the first one being the electronic ground state of CH_2 at the linear configuration, as expected from Hund's rule. However, the lower-energy Renner-Teller-split component arising from the $^1\Delta_g$ electronic state of CH_2 lies only slightly above its ground electronic state at bent geometries, as a result of strong Renner-Teller and pseudo-Renner-Teller vibronic interactions.

The calculation of accurate rovibronic spectra of CH_2 poses a considerable theoretical challenge due to its large-amplitude bending motion and the strong nonadiabatic couplings involved. Extensive calculations of the CH_2 spectra have previously been performed, based on a systematic treatment of the Renner-Teller vibronic coupling.[22–24] While the analysis of this effect has reached a high level of sophistication for the low-lying electronic states,[25] the treatment of the SO coupling in CH_2 is still largely phenomenological, as it is based on an effective SO coupling parameter between the $^1A_1$ and $^3B_1$ electronic states at bent geometries. This parameter is taken either as an empirical constant or is considered to be a function of the bending normal coordinate.[25]

Prototypical molecules in their own right are the halogenated derivatives of CH_2, i.e., CH(D)X and CX_2 with X=F, Cl, Br. They can be considered as model systems for the study of the spectroscopy and dynamics on three coupled potential energy surfaces, providing insight into the reactivity and electronic structure of carbenes as well as the interplay between SO coupling and Renner-Teller vibronic inter-

a)Electronic mail: ilias.sioutis@ch.tum.de.
b)Electronic mail: wolfgang.domcke@ch.tum.de.

actions. These species also serve as benchmarks for both theory and experiment. The ground electronic state of the dihalocarbenes, as well as of SiH_2 and GeH_2, corresponds to the lower Renner-Teller-split component of the $^1\Delta$ electronic state which is of $^1A_1$ spatial symmetry. The two lowest electronic states of CH(D)X are $\tilde{X}\,^1A'$ and $\tilde{A}\,^1A''$ at bent geometries. These arise from the Renner-Teller splitting of the electronically degenerate $^1\Delta$ ground electronic state at the linear configuration. The triplet electronic state with $^3A''$ spatial symmetry arises from the $^3\Sigma^-$ electronic state and lies in the vicinity of these Renner-Teller-split electronic states. The $\tilde{a}\,^3A''$ state plays a double role, as it is involved in SO coupling with the $\tilde{X}\,^1A'$ state and contributes to the perturbations of the $\tilde{A}\,^1A''$ electronic state of CH(D)X at the linear geometry.

The goal of the present work is the theoretical study of the interplay of the Renner-Teller and SO interactions in linear triatomic molecular systems with a half-filled π shell. While the combined effects of Σ-Π and SO vibronic couplings on the electronic structure of linear molecules have previously been investigated employing the microscopic (Breit-Pauli) spin-orbit coupling operator,[26,27] no corresponding information about the combined Σ-Δ and SO interactions has been elaborated thus far. We develop the theoretical formalism which is required for a systematic and comprehensive description of combined Renner-Teller and SO vibronic coupling effects in quasilinear molecules with a half-filled π orbital. We illustrate the effects of particular coupling terms by variational energy-level calculations for selected models. The carbenes as well as heavier linear triatomic species will be the systems of choice for the application of these methods. The results of the present analysis will facilitate a better understanding of the complicated perturbation mechanisms involved in these species as well as an unambiguous interpretation of the experimentally observed irregular patterns of their spin-vibronic energy levels which still defy a comprehensive spectroscopic analysis.

The remainder of this paper is arranged as follows. The derivation of the Hamiltonian and the analysis of its symmetry properties are reviewed. The effect of the Renner-Teller and other electrostatic vibronic-coupling parameters on the $^3\Sigma^-$, $^1\Delta$, and $^1\Sigma^+$ potential energy surfaces for a model molecular system is analyzed. The SO-induced vibronic coupling constants of the Hamiltonian are explicitly related to topographic features of these potential energy surfaces. Their impact on the $^3\Sigma^-$, $^1\Delta$, and $^1\Sigma^+$ spin-vibronic energy levels is discussed.

II. THEORY

A. Spin-vibronic Hamiltonian in the diabatic representation

Consider the two electrons of a half-filled π shell moving in the field of three linearly arranged nuclei along the z axis with effective nuclear charges Q_1, Q_2, and Q_3. The electronic states that arise from this electronic configuration are $^3\Sigma^-$, $^1\Delta$, and $^1\Sigma^+$. In this work, their mutual interaction and coupling due to the degenerate bending vibrational mode of π symmetry are examined. To simplify things, the effect of the two stretching vibrational modes on the vibronic coupling problem is not considered here. Their effect is to "tune" the energy separations among the $^3\Sigma^-$, $^1\Delta$, and $^1\Sigma^+$ electronic states. The present formalism can be extended to include the effects of the totally symmetric stretching vibrational modes, see, e.g., Refs. 27–29.

The spin-vibronic molecular Hamiltonian $\hat{\mathcal{H}}$ can be expressed as

$$\hat{\mathcal{H}} = \hat{T}_N + \hat{\mathcal{H}}_{\rm el} = \hat{T}_N + \hat{\mathcal{H}}_{\rm es} + \hat{\mathcal{H}}_{\rm SO}, \tag{1}$$

where $\hat{T}_N$ is the nuclear kinetic-energy operator and $\hat{\mathcal{H}}_{\rm el}$ is the electronic Hamiltonian which includes the kinetic energy of the electrons, the electron-nuclear and electron-electron interaction terms (represented by $\hat{\mathcal{H}}_{\rm es}$), as well as the SO interaction (given by $\hat{\mathcal{H}}_{\rm SO}$). If we express the dimensionless bending normal mode in the polar-coordinate representation (ρ, ϕ) and use atomic units, the nuclear kinetic-energy operator is given by

$$\hat{T}_N = -\frac{\omega}{2}\left[\frac{1}{\rho}\frac{\partial}{\partial\rho}\left(\rho\frac{\partial}{\partial\rho}\right) + \frac{1}{\rho^2}\frac{\partial^2}{\partial\phi^2}\right]. \tag{2}$$

The electrostatic part of the Hamiltonian is written as

$$\hat{\mathcal{H}}_{\rm es} = \sum_{m=1}^{2}\left(-\tfrac{1}{2}\boldsymbol{\nabla}_m^2 - \sum_{n=1}^{3}\frac{Q_n}{r_{mn}}\right) + \frac{1}{r_{12}}, \tag{3}$$

and the Breit-Pauli SO operator for two electrons is

$$\hat{\mathcal{H}}_{\rm SO} = \sum_{m=1}^{2}\hat{\mathcal{H}}_{\rm SO}^{(m)} + \hat{\mathcal{H}}_{\rm SO}^{(12)}, \tag{4}$$

where

$$\hat{\mathcal{H}}_{\rm SO}^{(m)} = \tfrac{1}{2}g\beta_e^2\hat{\mathbf{S}}_m\sum_{n=1}^{3}\frac{Q_n}{r_{mn}^3}(\mathbf{r}_{mn}\times(-i\boldsymbol{\nabla}_m)) \tag{5}$$

represents its one-electron part $(m=1,2)$ and

$$\hat{\mathcal{H}}_{\rm SO}^{(12)} = \frac{ig\beta_e^2}{2r_{12}^3}[\hat{\mathbf{S}}_1[\mathbf{r}_{12}\times(\boldsymbol{\nabla}_1 - 2\boldsymbol{\nabla}_2)] + \hat{\mathbf{S}}_2[\mathbf{r}_{21}\times(\boldsymbol{\nabla}_2 - 2\boldsymbol{\nabla}_1)]] \tag{6}$$

is the corresponding two-electron contribution.[30] Here, $g \simeq 2.0023$ refers to the g factor of the free electron and $\beta_e = 1/2c$ designates the Bohr magneton.

In Eq. (2), ω refers to the harmonic vibrational frequency of the bending vibrational mode. The normal coordinates of the bending vibrational mode $Q_\pm$ are given by the relationship

$$Q_\pm = Q_x \pm iQ_y = \rho e^{\pm i\phi}, \tag{7}$$

where (Q_x, Q_y) are the dimensionless bending normal coordinates. In Eqs. (5) and (6), $\mathbf{r}_1$ and $\mathbf{r}_2$ refer to the radius vectors of electrons 1 and 2, respectively, $\mathbf{R}_n$ $(n=1,2,3)$ correspond to the nuclear radius vectors, $\mathbf{r}_{mn}=\mathbf{r}_m-\mathbf{R}_n$ $(r_{mn}=|\mathbf{r}_{mn}|)$, $\mathbf{r}_{12}=\mathbf{r}_1-\mathbf{r}_2=-\mathbf{r}_{21}$ $(r_{12}=|\mathbf{r}_{12}|)$, and

$$\mathbf{S}_m = \mathbf{i}\hat{\sigma}_x^{(m)} + \mathbf{j}\hat{\sigma}_y^{(m)} + \mathbf{k}\hat{\sigma}_z^{(m)}. \tag{8}$$

In Eq. (8), $\hat{\sigma}_x^{(m)}$, $\hat{\sigma}_y^{(m)}$, and $\hat{\sigma}_z^{(m)}$ denote the Pauli spin matrices and **i**, **j**, and **k** symbolize the unit vectors of the three-dimensional space.

The symmetry properties of the electronic Hamiltonian $\hat{\mathcal{H}}_{\mathrm{el}}$ are represented by the commutators

$$[\hat{\mathcal{H}}_{\mathrm{el}}, \hat{\mathcal{J}}_z] = 0 \tag{9}$$

and

$$[\hat{\mathcal{H}}_{\mathrm{el}}, \hat{\mathcal{T}}] = 0, \tag{10}$$

where

$$\hat{\mathcal{J}}_z = \hat{\mathcal{L}}_z + \hat{\mathcal{S}}_z = -i\frac{\partial}{\partial\theta_1} + \tfrac{1}{2}\hat{\sigma}_z^{(1)} - i\frac{\partial}{\partial\theta_2} + \tfrac{1}{2}\hat{\sigma}_z^{(2)} \tag{11}$$

is the z component of the electronic (orbital+electron spin) angular momentum operator[31] and

$$\hat{\mathcal{T}} = \hat{\sigma}_y^{(1)}\hat{\sigma}_y^{(2)}\widehat{\mathrm{c.c.}} \tag{12}$$

stands for the time-reversal symmetry operator.[31,32] Here, θ represents the electronic azimuthal angular coordinate, $\hat{\sigma}_z^{(m)}$ corresponds to the z projection of the spin angular momentum of the mth electron, and $\widehat{\mathrm{c.c.}}$ denotes the operation of complex conjugation. $\hat{\mathcal{T}}$ is an antiunitary operator[31,32] and obeys the relation $\hat{\mathcal{T}}^2 = 1$ for molecular systems with an even number of electrons (as is the case here).

The full molecular Hamiltonian defined in Eq. (1) also possesses time-reversal symmetry and satisfies the axial symmetry property, i.e., it commutes with the z component of the total (electronic+nuclear) angular momentum operator, which is defined by

$$\hat{\mathcal{J}}_z' = \hat{\mathcal{J}}_z - i\frac{\partial}{\partial\phi}. \tag{13}$$

The eigenvalues of $\hat{\mathcal{J}}_z'$ are denoted by the spin-vibronic angular momentum quantum numbers μ and are integers ($\mu = 0, \pm 1, \pm 2, \ldots$). In the absence of SO coupling interactions, the electronic orbital (Λ) and electron spin (Σ) projection quantum numbers are good quantum numbers. In the presence of SO coupling, $\Omega = \Lambda + \Sigma$ is a good quantum number in the fixed-nuclei approximation. When the nuclear motion is included, only μ remains a good quantum number.

We introduce π-type molecular orbitals $P(r,z)e^{\pm i\theta}$ which are solutions of the one-electron (Hartree-Fock) Schrödinger equation at the linear configuration, where r, z, and θ represent cylindrical electronic coordinates. We define a two-electron diabatic[33–35] spin-orbital electronic basis set (diabatic spin orbitals) for a linear triatomic molecular system.[1–3] The basis set consists of the two electronic components of the $^1\Delta$ electronic state (with electronic orbital angular momentum quantum numbers $\Lambda = \pm 2$) and the electronic states corresponding to the $^3\Sigma^-$ and $^1\Sigma^+$ spatially nondegenerate electronic states ($\Lambda = 0$). Their spin angular momentum quantum numbers are $\Sigma = 0, \pm 1$.

The two-electron diabatic electronic basis functions ψ_Ω^Λ, which are orthonormal, antisymmetric with respect to electron exchange, and eigenfunctions of $\hat{S}^2$, $\hat{S}_z$, $\hat{L}_z$, and $\hat{J}_z$, are given by

$$\psi_{+2}^{+2} = \frac{1}{\sqrt{2}}P(1)P(2)e^{i(\theta_1+\theta_2)}(\alpha_1\beta_2 - \alpha_2\beta_1), \tag{14}$$

$$\psi_{+1}^{0} = \frac{1}{\sqrt{2}}P(1)P(2)[e^{i(\theta_1-\theta_2)} - e^{-i(\theta_1-\theta_2)}](\alpha_1\alpha_2), \tag{15}$$

$$\psi_{0}^{0} = \tfrac{1}{2}P(1)P(2)[e^{i(\theta_1-\theta_2)} - e^{-i(\theta_1-\theta_2)}](\alpha_1\beta_2 + \alpha_2\beta_1), \tag{16}$$

$$\phi_{0}^{0} = \tfrac{1}{2}P(1)P(2)[e^{i(\theta_1-\theta_2)} + e^{-i(\theta_1-\theta_2)}](\alpha_1\beta_2 - \alpha_2\beta_1), \tag{17}$$

$$\psi_{-1}^{0} = \frac{1}{\sqrt{2}}P(1)P(2)[e^{i(\theta_1-\theta_2)} - e^{-i(\theta_1-\theta_2)}](\beta_1\beta_2), \tag{18}$$

$$\psi_{-2}^{-2} = \frac{1}{\sqrt{2}}P(1)P(2)e^{-i(\theta_1+\theta_2)}(\alpha_1\beta_2 - \alpha_2\beta_1), \tag{19}$$

where $P(m) = P(r_m, z_m)$, m denotes the label of the electron, and (α,β) correspond to the two possible electron spin eigenfunctions. The wave functions defined in Eqs. (15), (16), and (18) are antisymmetric with respect to reflection through the molecular plane of the $D_{\infty h}$ or $C_{\infty v}$ point group, while the one defined in Eq. (17) is symmetric and is distinguished by the label ϕ. The above set of diabatic electronic basis functions is defined in the absence of interelectronic interactions.

The time-reversal operator $\hat{\mathcal{T}}$ has the following effects on the six diabatic electronic basis functions:

$$\hat{\mathcal{T}}(\psi_{\pm 2}^{\pm 2}) = -\psi_{\mp 2}^{\mp 2}\widehat{\mathrm{c.c.}} \tag{20}$$

$$\hat{\mathcal{T}}(\psi_{\pm 1}^{0}) = \psi_{\mp 1}^{0}\widehat{\mathrm{c.c.}} \tag{21}$$

$$\hat{\mathcal{T}}(\psi_{0}^{0}) = -\psi_{0}^{0}\widehat{\mathrm{c.c.}} \tag{22}$$

$$\hat{\mathcal{T}}(\phi_{0}^{0}) = -\phi_{0}^{0}\widehat{\mathrm{c.c.}}. \tag{23}$$

Hence, the time-reversal symmetry operator $\hat{\mathcal{T}}$ in the diabatic representation is given by

$$\hat{\mathcal{T}}\begin{pmatrix} \psi_{+2}^{+2} \\ \psi_{+1}^{0} \\ \psi_{0}^{0} \\ \phi_{0}^{0} \\ \psi_{-1}^{0} \\ \psi_{-2}^{-2} \end{pmatrix} = \begin{pmatrix} 0 & 0 & 0 & 0 & 0 & -1 \\ 0 & 0 & 0 & 0 & 1 & 0 \\ 0 & 0 & -1 & 0 & 0 & 0 \\ 0 & 0 & 0 & -1 & 0 & 0 \\ 0 & 1 & 0 & 0 & 0 & 0 \\ -1 & 0 & 0 & 0 & 0 & 0 \end{pmatrix} \begin{pmatrix} \psi_{+2}^{+2} \\ \psi_{+1}^{0} \\ \psi_{0}^{0} \\ \phi_{0}^{0} \\ \psi_{-1}^{0} \\ \psi_{-2}^{-2} \end{pmatrix} \widehat{\mathrm{c.c.}}. \tag{24}$$

Following the methodology of Refs. 1, 3, and 26, a 6×6 spin-vibronic Hamiltonian matrix can be derived in the six-dimensional spin-orbital electronic Hilbert space of the diabatic electronic basis functions defined in Eqs. (14)–(19). The matrix elements of $\hat{\mathcal{H}}_{\mathrm{el}}$ are expanded in a Taylor series in

TABLE I. The electrostatic (a and c) and SO-induced (g, d, d', and b) vibronic coupling coefficients of the bending vibrational mode that parametrize the model electronic Hamiltonian, defined in the diabatic electronic basis set, and their relationships to the terms of the Taylor series expansion of the potential.

Symbol	Description	Definition
a	Quartic Renner-Teller coupling coefficient	$\frac{1}{4!}\left(\frac{\partial^4}{\partial\rho^4}\langle\psi_{+2}^{+2}\vert\hat{\mathcal{H}}_{\mathrm{el}}\vert\psi_{+2}^{-2}\rangle\right)_0$
c	Quadratic $^1\Sigma^+-{}^1\Delta$ coupling coefficient	$\frac{1}{2!}\left(\frac{\partial^2}{\partial\rho^2}\langle\psi_{\pm2}^{\pm2}\vert\hat{\mathcal{H}}_{\mathrm{el}}\vert\phi_0^0\rangle\right)_0$
g	Zeroth-order $^3\Sigma_0^--{}^1\Sigma_0^+$ coupling coefficient	$(\langle\psi_0^0\vert\hat{\mathcal{H}}_{\mathrm{SO}}\vert\phi_0^0\rangle)_0$
d	Linear $^3\Sigma_{\pm1}^--{}^1\Delta_{\pm2}$ coupling coefficient	$\left(\frac{\partial}{\partial\rho}\langle\psi_{\pm2}^{\pm2}\vert\hat{\mathcal{H}}_{\mathrm{SO}}\vert\psi_{\pm1}^0\rangle\right)_0$
d'	Linear $^3\Sigma_{\pm1}^--{}^1\Sigma_0^+$ coupling coefficient	$\left(\frac{\partial}{\partial\rho}\langle\psi_{\pm1}^0\vert\hat{\mathcal{H}}_{\mathrm{SO}}\vert\phi_0^0\rangle\right)_0$
b	Cubic $^3\Sigma_{\mp1}^--{}^1\Delta_{\pm2}$ coupling coefficient	$\frac{1}{3!}\left(\frac{\partial^3}{\partial\rho^3}\langle\psi_{\pm2}^{\pm2}\vert\hat{\mathcal{H}}_{\mathrm{SO}}\vert\psi_{\mp1}^0\rangle\right)_0$

the bending amplitude ρ, keeping expansion terms up to fourth order in ρ. Angular momentum conservation and time-reversal symmetry determine the nonvanishing matrix elements. A further simplification is achieved by the explicit calculation of the individual coefficients, performing the integration over the angular variables θ_1 and θ_2 as well as over the discrete spin variables (see, e.g., Ref. 3). More details are given in Appendix A. The result of this derivation is

$$\hat{\mathcal{H}}=\hat{\mathcal{T}}_N+\hat{\mathcal{H}}_{\mathrm{el}}=\left(\hat{\mathcal{T}}_N+\frac{1}{2}\omega\rho^2+\frac{1}{4!}\lambda\rho^4\right)\mathbf{1}+\begin{bmatrix} E^{1}\Delta_{+2} & d\rho e^{i\phi} & 0 & c\rho^2e^{2i\phi} & b\rho^3e^{3i\phi} & a\rho^4e^{4i\phi} \\ d\rho e^{-i\phi} & E^{3}\Sigma_{+1}^- & 0 & d'\rho e^{i\phi} & 0 & -b\rho^3e^{3i\phi} \\ 0 & 0 & E^{3}\Sigma_0^- & g & 0 & 0 \\ c\rho^2e^{-2i\phi} & d'\rho e^{-i\phi} & g & E^{1}\Sigma_0^+ & -d'\rho e^{i\phi} & c\rho^2e^{2i\phi} \\ b\rho^3e^{-3i\phi} & 0 & 0 & -d'\rho e^{-i\phi} & E^{3}\Sigma_{-1}^- & -d\rho e^{i\phi} \\ a\rho^4e^{-4i\phi} & -b\rho^3e^{-3i\phi} & 0 & c\rho^2e^{-2i\phi} & -d\rho e^{-i\phi} & E^{1}\Delta_{-2} \end{bmatrix}, \tag{25}$$

where $\mathbf{1}$ represents the 6×6 unit matrix and λ denotes the quartic anharmonic-oscillator parameter.

$(E^1\Delta_{+2};E^1\Delta_{-2})$, $(E^3\Sigma_{+1}^-;E^3\Sigma_0^-;E^3\Sigma_{-1}^-)$, and $E^1\Sigma_0^+$ correspond to the energies of the $^1\Delta$, $^3\Sigma^-$, and $^1\Sigma^+$ SO-coupled electronic states at the linear geometry ($\rho=0$), respectively. The energy separations between the $^3\Sigma^-$ and $^1\Delta$ potential energy surfaces as well as between the $^1\Delta$ and $^1\Sigma^+$ states at $\rho=0$ are designated as $\mathcal{E}_1$ and $\mathcal{E}_2$, respectively, in the following. While the vibronic parameters a (quartic Renner-Teller coupling between the two electronic components of $^1\Delta$) and c (quadratic $^1\Sigma^+-{}^1\Delta$ coupling) are of nonrelativistic (electrostatic) character, the parameters g (zeroth-order $^3\Sigma_0^--{}^1\Sigma_0^+$ coupling), d (linear $^3\Sigma_{\pm1}^--{}^1\Delta_{\pm2}$ coupling), d' (linear $^3\Sigma_{\pm1}^--{}^1\Sigma_0^+$ coupling), and b (cubic $^3\Sigma_{\pm1}^--{}^1\Delta_{\mp2}$ coupling) are of SO origin. The effects of the zeroth-, first-, second-, third-, and fourth-order vibronic coupling parameters on the topography of the potential energy surfaces will be discussed below. The definitions of the SO-induced, Renner-Teller, and $^1\Sigma^+-{}^1\Delta$ interstate vibronic coupling parameters are summarized in Table I. Note that most of the SO-induced coupling parameters would be absent if a phenomenological expression of the SO coupling operator[36,37] were used instead. Equation (25) reveals, in particular, that the Breit-Pauli SO operator is not diagonal in the diabatic electronic basis.

Among all vibronic coupling matrix elements, the parameter g is the only one which has an effect on the potential energy surfaces at the linear geometry. Specifically, it couples the $^3\Sigma^-$ state with the $^1\Sigma^+$ state. As a result of this coupling, the spin degeneracy of the $^3\Sigma^-$ state is lifted (see Sec. III B for details). It has previously been shown that nonzero SO matrix elements exist between Σ states with different multiplicities ($\Delta S=1$) when these behave differently under the σ_v operation.[30] The SO coupling does not lift the degeneracy of the $^1\Delta$ state at $\rho=0$ in conformity with group theoretical considerations. The SO-coupled electronic Hamiltonian matrix of Eq. (25) can be diagonalized for $\rho=0$ by a

constant (ρ- and ϕ-independent) unitary transformation. The vibronic matrix presumably cannot be transformed to a block-diagonal form for $\rho \neq 0$.

B. Vibronic basis set and vibronic eigenfunctions

The basis set used for the variational calculation of vibronic energy levels corresponds to direct products of electronic and vibrational wave functions (spin-vibronic basis set) and is represented by

$$|\Lambda,\Sigma,n,l\rangle = |\Lambda,\Sigma\rangle|n,l\rangle, \tag{26}$$

with electronic quantum numbers $\Lambda=0, \pm 2$, $\Sigma=0, \pm 1$, and vibrational quantum numbers $n=0,1,2,\ldots$, $l=n, n-2,\ldots, -n+2, -n$. The electronic wave functions $|\Lambda,\Sigma\rangle$ refer to the spin-orbital diabatic electronic basis set defined in Eqs. (14)–(19), while the $|n,l\rangle$ are the eigenfunctions of the two-dimensional isotropic harmonic oscillator.[38]

Since $[\hat{\mathcal{H}},\hat{\mathcal{J}}_z']=0$, the vibronic eigenfunctions can be classified by the spin-vibronic quantum number μ,

$$\hat{\mathcal{J}}_z' \psi_\mu = \mu \psi_\mu. \tag{27}$$

The spin-vibronic basis set of Eq. (26) is constructed by first specifying the electronic angular momentum quantum numbers Ω and then selecting suitable values of l of the $|n,l\rangle$ vibrational wave functions for a given value of μ.

The spin-vibronic eigenfunctions with total angular momentum quantum number μ, ψ_μ, satisfy the Schrödinger equation

$$\hat{\mathcal{H}}\psi_\mu = E\psi_\mu \tag{28}$$

for $\hat{\mathcal{H}}$ of Eq. (1). They are expressed as linear combinations of the basis functions (26) for a given quantum number μ. A second quantum number n_μ is used to label the eigenvalues (ordered by increasing energy) for a given μ. We, thus, denote eigenkets as $|\mu,n_\mu\rangle$.

Based on the above, the spin-vibronic eigenfunctions $|\mu,n_\mu\rangle$ may be written as

$$|\mu,n_\mu\rangle = \sum_k C_k^{n\mu} |\Lambda\rangle|\Sigma\rangle|n,l\rangle, \tag{29}$$

where the index k of the expansion coefficients $C_k^{n\mu}$ represents all symmetry-allowed combinations of the basis-set quantum numbers Λ, Σ, n, and l. To simplify the notation, we shall hereafter drop the $\pm$ signs of the μ quantum numbers.

Equation (26) defines a complete basis set. The basis set must be truncated to some manageable size for the numerical diagonalization of the Hamiltonian matrix. The calculated eigenvalues are tested for convergence by systematically increasing the number of vibrational basis functions until additional basis functions have a negligible effect on the eigenvalues. The final matrices used were of the order of 10^3. The nonvanishing matrix elements of the spin-vibronic Hamiltonian are given in Appendix B.

III. RESULTS AND DISCUSSION

The concept of the electronic adiabatic potential energy surface (PES) is well-defined when the Born-Oppenheimer approximation is valid, particularly if SO coupling is not relevant for the problem. The Renner-Teller effect is an exemplary case of a breakdown of the Born-Oppenheimer approximation. However, it is still useful to use the concept of the adiabatic PESs for Renner-Teller active molecules in the presence of SO coupling. In the following, the topographies of two types of adiabatic PESs will be described. The first type refers to the eigenvalues of $\hat{\mathcal{H}}_{\rm es}$ (Sec. III A), while the second corresponds to the eigenvalues of $\hat{\mathcal{H}}_{\rm es}+\hat{\mathcal{H}}_{\rm SO}$ (Secs. III B and III C). The PESs are obtained as parametric functions of the nuclear positions by numerical diagonalization of the 6×6 Hamiltonian matrix (we did not succeed in obtaining analytical expressions for the eigenvalues even with the aid of symbolic-mathematical tools).

We also investigate the effects of SO-induced vibronic coupling interactions (Sec. III B) as well as the combined effects of Renner-Teller, $^1\Sigma^+-{}^1\Delta$, and SO-induced coupling (Sec. III C) on the spin-vibronic energy levels of the $^3\Sigma^-$, $^1\Delta$, and $^1\Sigma^+$ electronic states for representative parameter values. Since the Renner-Teller and $^1\Sigma^+-{}^1\Delta$ electrostatic couplings have a negligible impact on the energy-level diagrams for reasonable parameter values, they will not be considered any further in the present study.

A. Hamiltonian without SO coupling

The effects of the quartic $^1\Delta$ Renner-Teller and quadratic $^1\Sigma^+-{}^1\Delta$ electrostatic vibronic coupling mechanisms on the adiabatic PESs of the $^3\Sigma^-$, $^1\Delta$, and $^1\Sigma^+$ electronic states of a linear triatomic molecule are illustrated in Fig. 1. The figure displays cross sections of the PESs (for any azimuthal angle ϕ) along the dimensionless bending normal coordinate ρ for a system with the parameters $\mathcal{E}_1=\mathcal{E}_2=5\omega$ and $\lambda/\omega=0.2$ in the limit of vanishing SO coupling interactions. The parameters were expressly chosen to highlight the effect of the involved coupling mechanisms on the adiabatic PESs; that is, comparatively large values of the coupling parameters were chosen. Note that the ordinate scale of these diagrams is in units of ω and that the energy of the $^3\Sigma^-$ state, i.e., $E_{^3\Sigma^-}$, is 0 for $\rho=0$.

The lowest curve (near $\rho=0$) represents a slice across the $^3\Sigma^-$ PES. The next-lowest function gives the $^1\Delta$ PES, while the uppermost curve depicts the $^1\Sigma^+$ PES. The energy ordering of these potential energy curves is based on Hund's rule. The $^3\Sigma^-$ potential is threefold spin degenerate. The $^1\Sigma^+$ PES is nondegenerate, while the $^1\Delta$ PES retains its twofold electronic degeneracy only in the limit of vanishing Renner-Teller coupling and $^1\Sigma^+-{}^1\Delta$ quadratic vibronic coupling. The Renner-Teller theory predicts[39,40] that a $^1\Delta$ electronic state of a linear molecule will interact with the π vibration in fourth order, leading to two PESs which touch at the linear configuration.

The PESs of Fig. 1(a) were constructed considering only the quartic Renner-Teller vibronic coupling effect, assuming $a/\omega=0.01$. Upon displacement from the linear geometry ($\rho=0$) along the bending coordinate, the $^3\Sigma^-$, $^1\Delta$, and $^1\Sigma^+$ elec-

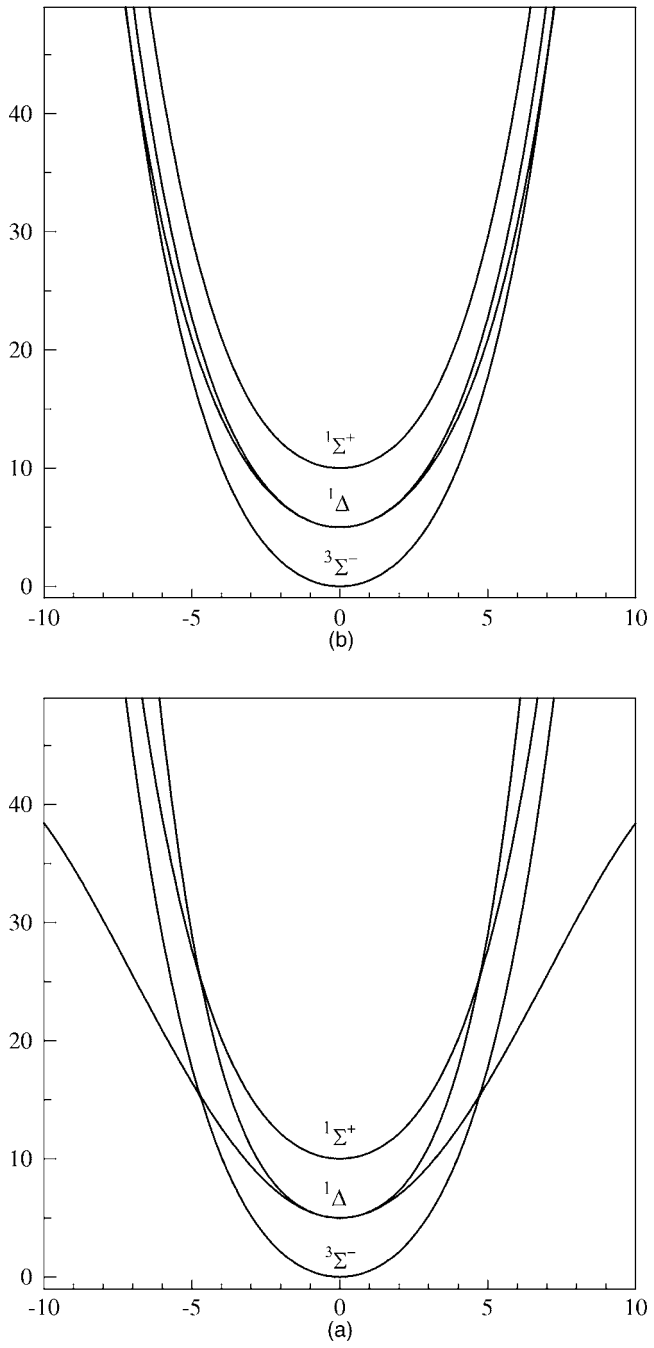

FIG. 1. Potential energy as a function of the bending coordinate for selected cases of Renner-Teller and $^1\Sigma^+-{}^1\Delta$ electrostatic vibronic couplings for Σ and Δ electronic states of quasilinear triatomic molecules with a half-filled π shell. The ordinate scale is in units of ω, while the abscissa represents the dimensionless bending normal coordinate ρ. The curves shown here have been constructed for $\mathcal{E}_1=\mathcal{E}_2=5\omega$ and $\lambda/\omega=0.2$. The energy $E_{^3\Sigma^-}$ is defined as 0 for $\rho=0$. (a) Renner-Teller vibronic coupling of the two electronic components of $^1\Delta$ ($a/\omega=0.01$; $\lambda/\omega=0.2$; $c/\omega=0$). (b) Quadratic vibronic coupling of $^1\Sigma^+$ and $^1\Delta$ ($c/\omega=0.1$; $\lambda/\omega=0.2$; $a/\omega=0$).

tronic states reduce to $^3B_1$, ($^1A_1$, $^1B_1$) and $^1A_1$ in C_{2v} geometry, respectively. (Note that an in-plane y axis is assumed in this work.) As the Renner-Teller effect becomes stronger, the interaction between the two $^1\Delta$ electronic components increases; the splitting between them becomes more pronounced and starts at smaller displacements from the reference geometry (not shown). Note the crossing between the $^1\Delta$ Renner-Teller-split potential energy functions with the $^3\Sigma^-$ and $^1\Sigma^+$ functions at $\rho\approx\pm4.5$ in Fig. 1(a). The Renner-Teller splitting of the electronically degenerate $^1\Delta$ PESs, being a fourth-order effect, is expected to take place at larger displacements from the linear geometry than for Π-type Renner-Teller-split PESs. The slice across the lowest sheet of the $^1\Delta$ PESs exhibits a double-well topography if the parameter a/ω exceeds a certain critical value.

Figure 1(b) exhibits the ramifications of the $^1\Sigma^+-{}^1\Delta$ quadratic electrostatic interaction on the PESs for the example case of $c/\omega=0.1$. Only the shapes of the $^1\Sigma^+$ and $^1\Delta$ PESs are expected to change, as this interaction does not involve vibronic coupling with the $^3\Sigma^-$ electronic state. The $^1\Sigma^+-{}^1\Delta$ interaction removes the degeneracy of the $^1\Delta$ components.

B. Hamiltonian with SO coupling, excluding electrostatic vibronic coupling

1. Potential energy surfaces

Figure 2 is constructed based on the same general principles which have been applied for Fig. 1, but now the pure SO-induced vibronic coupling effects are considered. Specifically, the diagrams (a)–(d) of Fig. 2 examine the effects of the zeroth-order ($g/\omega=6$), first-order ($d/\omega=2$), ($d'/\omega=2$), and third-order ($b/\omega=0.1$) SO-induced vibronic coupling interactions on the $^3\Sigma^-$, $^1\Delta$, and $^1\Sigma^+$ PESs, respectively (the parameter values are given in the caption). The parameter values were chosen with the express purpose of illustrating and enhancing the SO-induced vibronic coupling effects.

Let us first examine the implications of the zeroth-order $^3\Sigma_0^-{}-{}^1\Sigma_0^+$ SO vibronic coupling parameter g for these PESs. If we assume a linear geometry ($\rho=0$), then the 6×6 electronic Hamiltonian matrix of Eq. (25) decouples into a diagonal matrix and a 2×2 submatrix which is responsible for the mixing of the $^3\Sigma_0^-$ and $^1\Sigma_0^+$ electronic states. The electronic states $^1\Delta_{\pm2}$ and $^3\Sigma_{\pm1}^-$ retain their twofold degeneracies and their potentials remain unaffected.

The linear (first order in ρ) SO-induced vibronic coupling parameters d and d' are expected to have, apart from the zeroth-order parameter g, the largest impact on the topography of the $^3\Sigma^-$, $^1\Delta$, and $^1\Sigma^+$ PESs. We first investigate the effect of the parameter d which refers to the coupling between $^3\Sigma_{\pm1}^-$ and $^1\Delta_{\pm2}$. If we assume that all parameters except d are zero, then the 6×6 electronic Hamiltonian matrix of Eq. (25) reduces to two 2×2 submatrices which mix (for $\rho\neq0$) the $^1\Delta_{\pm2}$ and $^3\Sigma_{\pm1}^-$ electronic states. The $^3\Sigma_0^-$ and $^1\Sigma_0^+$ electronic states remain unaffected. While the twofold degeneracies of the $^3\Sigma_{\pm1}^-$ and $^1\Delta_{\pm2}$ PESs are retained, their curvatures change. The $^3\Sigma_{\pm1}^-$ PES develops a double-minimum shape along the bending normal coordinate, while the $^1\Delta_{\pm2}$ function becomes steeper as a function of ρ upon increase of d/ω [see Fig. 2(b)]. As d' involves the $^3\Sigma_{\pm1}^-$ and $^1\Sigma_0^+$ electronic states, the vibronic coupling interaction is now manifested between the $^3\Sigma_{\pm1}^-$ and $^1\Sigma^+$ PESs. If we assume that all parameters except d' are zero, then the 6×6 electronic Hamiltonian matrix of Eq. (25) reduces to a 4×4 submatrix which mixes (for $\rho\neq0$) the $^3\Sigma_{\pm1}^-$ and $^1\Sigma_0^+$ electronic states. The $^1\Sigma^+$ well is compressed and the $^3\Sigma_{\pm1}^-$ PES exhibits a flattening, while retaining its double degen-

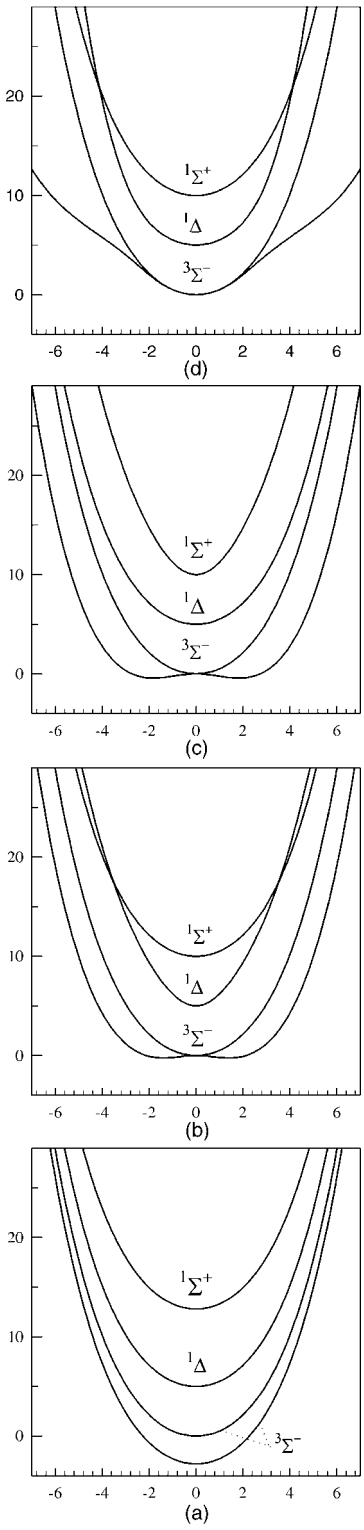

FIG. 2. Potential energy as a function of the bending coordinate for selected cases of SO-induced vibronic coupling in Σ and Δ electronic states of quasilinear triatomic molecules with a half-filled π shell. The ordinate scale is in units of ω, while the abscissa represents the dimensionless bending normal coordinate ρ. The curves shown here have been constructed for $\mathcal{E}_1=\mathcal{E}_2=5\omega$ and $\lambda/\omega=0.2$. The energy $E^{3}\Sigma^-$ is defined as 0 for $\rho=0$. The diagrams (a)–(d) represent "large" vibronic interactions: (a) zeroth-order vibronic coupling of $^3\Sigma_0^-$ and $^1\Sigma_0^+$ ($g/\omega=6$; $\lambda/\omega=0.2$; $d/\omega=0$; $d'/\omega=0$; $b/\omega=0$), (b) linear vibronic coupling of $^3\Sigma_{\pm1}^-$ and $^1\Delta_{\pm2}$ ($d/\omega=2$; $\lambda/\omega=0.2$; $g/\omega=0$; $d'/\omega=0$; $b/\omega=0$), (c) linear vibronic coupling of $^3\Sigma_{\pm1}^-$ and $^1\Sigma_0^+$ ($d'/\omega=2$; $\lambda/\omega=0.2$; $g/\omega=0$; $d/\omega=0$; $b/\omega=0$), and (d) cubic vibronic coupling of $^3\Sigma_{\pm1}^-$ and $^1\Delta_{\mp2}$ ($b/\omega=0.1$; $\lambda/\omega=0.2$; $g/\omega=0$; $d/\omega=0$; $d'/\omega=0$).

eracy upon displacement from the linear geometry [see Fig. 2(c)]. The $^1\Delta$ potential remains unaltered. The $^3\Sigma_{\pm1}^-$ PES exhibits similar topographical characteristics in Figs. 2(c) and 2(b) since the parameter values of d'/ω and d/ω are the same in both cases. Of fundamental importance for kinetics and spectroscopic studies is the accurate determination of the barrier to linearity of the lowest PES which is defined as the energy difference between the bent equilibrium geometry and the "transition-state" linear geometry.

While the effect of the cubic SO-induced vibronic coupling parameter b on the $^3\Sigma^-$ and $^1\Delta$ PESs is less important than that of the zeroth-order and first-order contributions, it introduces interesting changes to the topographies of these PESs. This parameter represents third-order vibronic coupling between $^3\Sigma_{\pm1}^-$ and $^1\Delta_{\mp2}$. When all coupling parameters except b are zero, the 6×6 electronic Hamiltonian matrix of Eq. (25) reduces to a 4×4 submatrix which mixes (for $\rho\neq0$) the $^1\Delta_{\pm2}$ and $^3\Sigma_{\mp1}^-$ diabatic electronic states. The qualitative characteristics of this interaction are depicted in Fig. 2(d), where one can notice that one component of the $^3\Sigma^-$ PES becomes flatter upon bending, while the $^1\Delta_{\pm2}$ PES becomes steeper. The potentials of the $^3\Sigma_0^-$ and $^1\Sigma_0^+$ states remain unperturbed.

2. Spin-vibronic energy levels

Central to this work is the impact that the linear SO-induced vibronic coupling parameters d and d' have on the $^3\Sigma^-$, $^1\Delta$, and $^1\Sigma^+$ spin-vibronic energy levels. Figures 3(A) and 3(B) show the energy-level diagrams of the spin-vibronic energy levels with calculated energies lower than 5ω. The molecular parameters d/ω in (A) and d'/ω in (B) vary between 0 and 0.5. The energy levels were computed assuming $\mathcal{E}_1=1.5\omega$, $\mathcal{E}_2=1.8\omega$, and $\lambda/\omega=0$. The ordinate scales of the diagrams of (A) and (B) are in units of ω, while their abscissae refer to the dimensionless parameters d/ω and d'/ω, respectively. The solid, long-dashed, dash-dotted, dotted and medium-dashed lines correspond to energy levels with $\mu=0$, 1, 2, 3, and 4, respectively. The symmetry labels of the states were determined in the same way as in Ref. 36. Note the correlation of the spin-vibronic energy levels with the harmonic-oscillator vibronic energy levels, as well as the electronic states from which the latter levels arise in panels (A) and (B) of Fig. 3.

As the linear SO-induced vibronic interaction parameter d involves coupling between the electronic states $^3\Sigma^-$ and $^1\Delta$, we expect energy-level perturbations to take place among their energy levels satisfying $\Delta v=1$. The degeneracy of the lowest two $\mu=0$, 1 ($^3\Sigma^-, v=0$) spin-vibronic energy levels in (A) is lifted since the latter one interacts with the $\mu=1$ ($^1\Delta, v=1$) energy level. The former energy level remains unperturbed as there is no ($^1\Delta, v=1$) energy level with $\mu=0$ to interact with. Similarly, the $\mu=2$ ($^1\Delta, v=0$) energy level interacts with the $\mu=2$ ($^3\Sigma^-, v=1$) energy level. [Note that this $^1\Delta$ level can cross with the $\mu=1,3$ $^3\Sigma^-$ levels as shown in Fig. 3(A)]. The ($^1\Delta, v=1$) energy levels with $\mu=3,1$ interact with the same-μ quantum-number ($^3\Sigma^-, v=2$) levels. Finally, the $\mu=4$, 2, and 0 ($^1\Delta, v=2$) energy levels interact with the $\mu=4$, 2, and 0 ($^3\Sigma^-$, $v=3$, 3, and 1, 3) levels, respectively. The same principles apply in Fig. 3(B), where

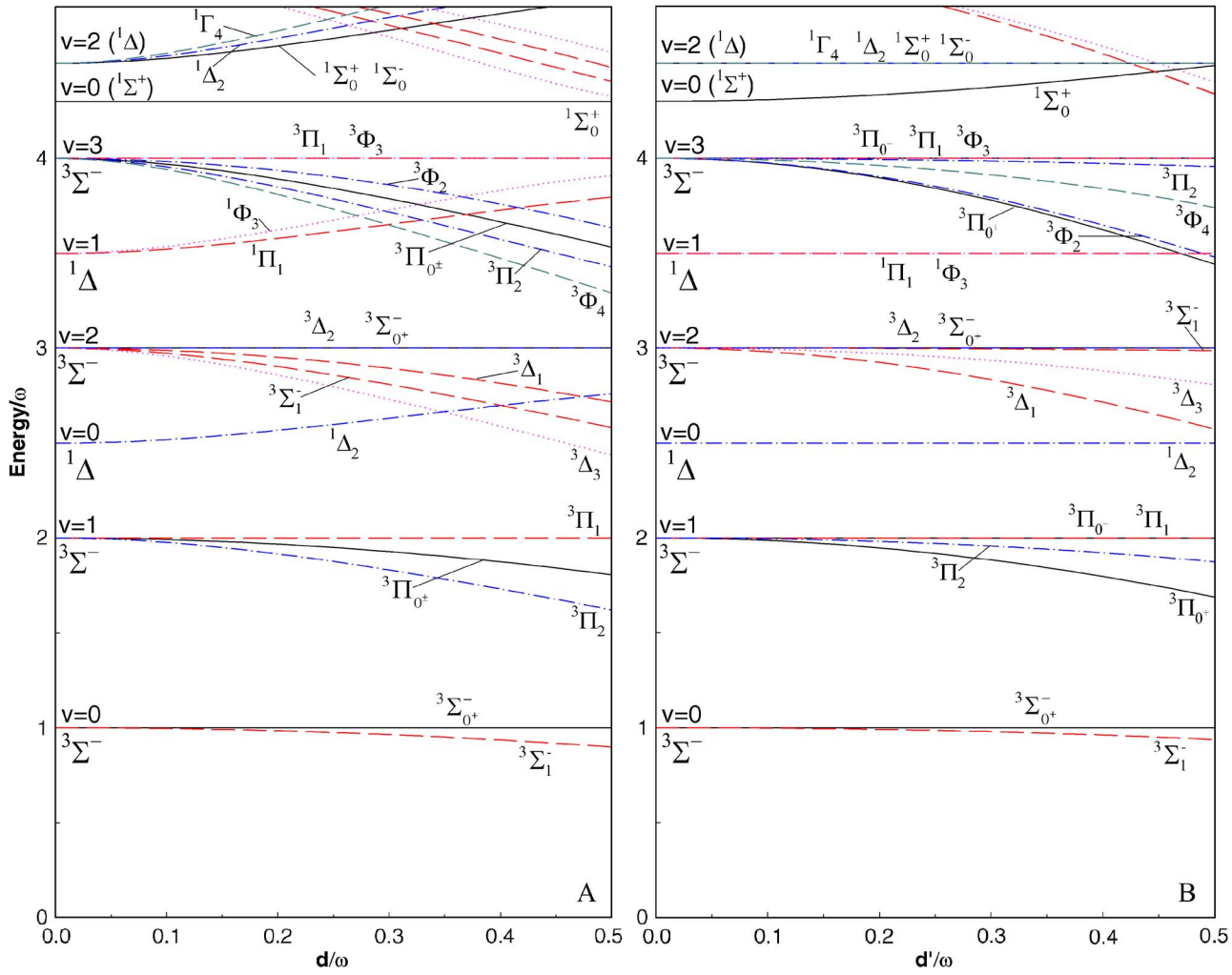

FIG. 3. (Color online) Calculated spin-vibronic energy levels with energies lower than 5ω of the $^3\Sigma^-$, $^1\Delta$, and $^1\Sigma^+$ electronic states for (A) linear $^3\Sigma^-_{\pm1}-{}^1\Delta_{\pm2}$ SO vibronic coupling (d) and (B) linear $^3\Sigma^-_{\pm1}-{}^1\Sigma^+_0$ SO vibronic coupling (d'), as a function of d/ω and d'/ω, respectively. The ordinate scale is in units of ω, while the abscissae in (A) and (B) refer to the dimensionless quantities d/ω and d'/ω, respectively. The solid, long-dashed, dash-dotted, dotted, and medium-dashed lines represent energy levels with $\mu=0$, 1, 2, 3, and 4, respectively. The energy levels were calculated for $\mathcal{E}_1=1.5\omega$, $\mathcal{E}_2=1.8\omega$, and $\lambda/\omega=0$.

the SO-induced vibronic coupling takes place between the $^3\Sigma^-$ and $^1\Sigma^+$ electronic states. For example, the lowest $\mu=1$ ($^3\Sigma^-, v=0$) energy level interacts with the $\mu=1$ ($^1\Sigma^+, v=1$) energy level, while the $\mu=0$ ($^3\Sigma^-, v=0$) energy level remains unaffected, as there is no $\mu=0$ ($^1\Sigma^+, v=1$) energy level to interact with. What is new in Fig. 3(B) is that only one of the two degenerate $\mu=0$ $^3\Sigma^-$ (shown for $v=1$ and 3) energy-level components may interact with suitable $^1\Sigma^+$ energy levels due to the d' spin-vibronic coupling.

Figure 4 illustrates the effects of third-order (parameter b) SO vibronic coupling on the $^3\Sigma^-$, $^1\Delta$, and $^1\Sigma^+$ spin-vibronic energy levels. This figure was constructed based on the same principles as applied for Figs. 3(A) and 3(B). All spin-vibronic energy levels with calculated energies lower than 5ω are retained in the diagram. The parameter b/ω varies in the range of (0,0.10). Figure 4 displays interesting higher-order spin-vibronic coupling effects. The increase of the parameter b/ω causes degenerate groups of energy levels to fully resolve into their individual components. What is unique here is the early onset of extensive interstate energy-level interactions. For example, the lowest $\mu=2$ ($^1\Delta, v=0$) energy level interacts with the $\mu=2$ ($^3\Sigma^-, v=1,3$) energy levels, and the variation of their energies reflects the counterbalance of these interactions.

The interaction pattern of the spin-vibronic energy levels is relatively trivial when the g parameter is varied. An important observation is that the energy-level perturbations become relevant already for small values of g/ω. Since g is of zeroth order in ρ (that is, purely electronic), it can become significantly larger than the bending vibrational frequency ω in molecules with heavy atoms.

C. Hamiltonian with SO coupling, Renner-Teller coupling, and $^1\Sigma^+-{}^1\Delta$ coupling

1. Potential energy surfaces

Figure 5 illustrates the combined effects of Renner-Teller, $^1\Sigma^+-{}^1\Delta$ electrostatic, and SO-induced vibronic coupling interactions on the $^3\Sigma^-$, $^1\Delta$, and $^1\Sigma^+$ PESs of a triatomic linear molecule for selected parameter values. The cross sections along the bending normal coordinate cover the most important regions of the $^3\Sigma^-$, $^1\Delta$, and $^1\Sigma^+$ PESs, such

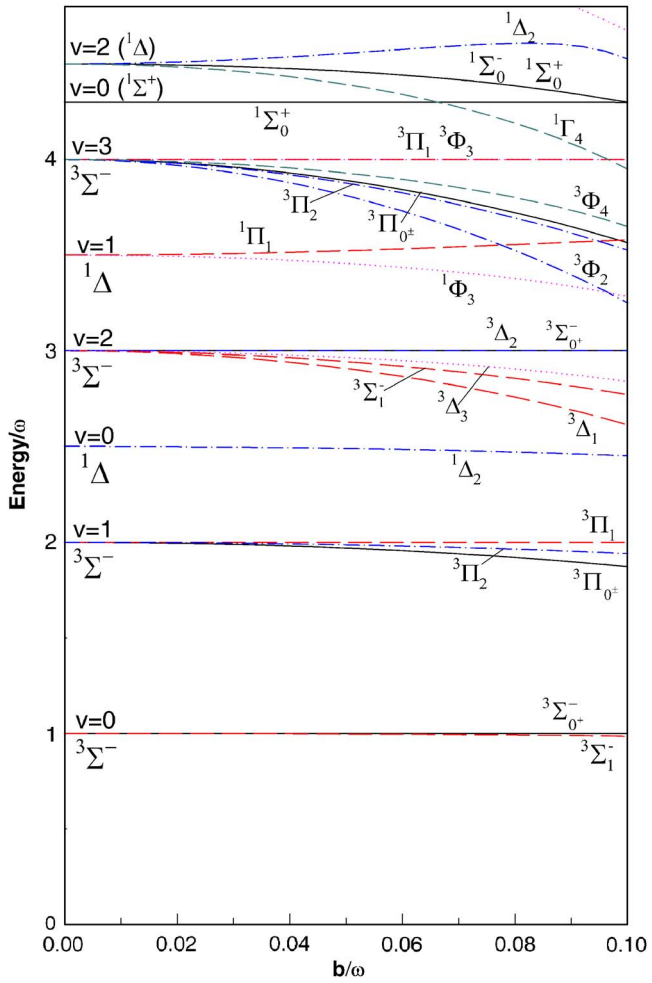

FIG. 4. (Color online) Calculated spin-vibronic energy levels with energies lower than 5ω of the $^3\Sigma^-$, $^1\Delta$, and $^1\Sigma^+$ electronic states for cubic $^3\Sigma^-_{\pm1}-{}^1\Delta_{\mp2}$ SO vibronic coupling (b) as a function of b/ω. The ordinate scale is in units of ω, while the abscissa refers to the dimensionless quantity b/ω. The solid, long-dashed, dash-dotted, dotted, and medium-dashed lines represent energy levels with $\mu=0$, 1, 2, 3, and 4, respectively. The energy levels were calculated assuming $\mathcal{E}_1=1.5\omega$, $\mathcal{E}_2=1.8\omega$, and $\lambda/\omega=0$.

as the stationary points of bent-geometry energy minima as well as linear-geometry local minima or local maxima.

Figure 5(a) was computed considering the zeroth-order $^3\Sigma^-_0-{}^1\Sigma^+_0$ SO coupling effect ($g/\omega=4$) plus the linear vibronic coupling between $^3\Sigma^-_{\pm1}$ and $^1\Sigma^+_0$ ($g/\omega=4$; $d'/\omega=2$). Figure 5(b) incorporates the same interactions as Fig. 5(a) plus the linear $^3\Sigma^-_{\pm1}-{}^1\Delta_{\pm2}$ vibronic coupling interaction ($g/\omega=4$; $d'/\omega=2$; $d/\omega=2$). Figure 5(c), finally, combines the topographic potential-energy-surface characteristics of the $^3\Sigma^-$, $^1\Delta$, and $^1\Sigma^+$ electronic states of Fig. 5(b) with those introduced by cubic SO vibronic coupling between $^3\Sigma^-_{\pm1}$ and $^1\Delta_{\mp2}$ ($g/\omega=4$; $d'/\omega=2$; $d/\omega=2$; $b/\omega=0.1$).

Once the linear SO coupling interaction (parameter d) is included in Fig. 5(b), a number of interesting effects become visible. What distinguishes Fig. 5(b) from Fig. 5(a) is that in the former figure, the twofold degeneracies of the $^3\Sigma^-_{\pm1}$ and $^1\Delta_{\pm2}$ PESs are fully resolved, which would not have taken place if the d and d' linear coupling effects were considered independently, as was done in Sec. III B. The combined effects of the d and d' linear couplings translate into a concomitant interaction between the $^3\Sigma^-_{\pm1}$ and the $^1\Delta_{\pm2}$ and $^1\Sigma^+_0$ PESs.

The interaction between the $^3\Sigma^-_{\pm1}$ and $^1\Delta_{\pm2}$ PESs is further enhanced by the inclusion of the cubic coupling term (b), as shown in Fig. 5(c). There appear two different sets of bent-geometry stationary points, those that correlate with the lowest of the two $^3\Sigma^-_{\pm1}$ PESs, which are located at $\rho\approx\pm6$, and the stationary points of the $^3\Sigma^-_0$ PES, which are positioned at $\rho\approx\pm2$.

Any combination of the linear and cubic vibronic coupling interactions, or the combined effects of the linear coupling interactions alone, leads to SO splitting of the degenerate components of the $^3\Sigma^-_{\pm1}$ and $^1\Delta_{\pm2}$ PESs. Consider the exemplary case of combined d and d' interactions. The former concerns the $^1\Delta_{\pm2}-{}^3\Sigma^-_{\pm1}$ coupling, whereas the latter refers to the $^1\Sigma^+_0-{}^3\Sigma^-_{\pm1}$ coupling. The d and d' effects are "competing" for the $^3\Sigma^-_{\pm1}$ energies. Therefore, the d vibronic coupling quenches the d' vibronic coupling and vice versa.

The joint action of Renner-Teller, $^1\Sigma^+-{}^1\Delta$ electrostatic, and SO-induced vibronic coupling effects on the $^3\Sigma^-$, $^1\Delta$, and $^1\Sigma^+$ PESs is illustrated in Fig. 5(d) which combines the effects of Fig. 5(c) plus the Renner-Teller and $^1\Sigma^+-{}^1\Delta$ electrostatic vibronic coupling ($a/\omega=0.002$; $c/\omega=0.04$; $g/\omega=4$; $d'/\omega=2$; $d/\omega=2$; $b/\omega=0.1$). Note the small, but non-negligible, repositioning of the local energy minima of the lowest $^3\Sigma^-_{\pm1}$ PES in Fig. 5(d) (at $\rho\approx\pm7$). Overall, one may conclude that the Renner-Teller and $^1\Sigma^+-{}^1\Delta$ electrostatic effects play only a moderate role for the shape of the PESs, while the SO-induced vibronic coupling effects have a determining impact on these.

2. Spin-vibronic energy levels

The purpose of Fig. 6 is to illustrate, through the results of numerical computations for a model system, how the combined effects of the SO-induced vibronic coupling terms of the vibronic Hamiltonian translate into energy-level interactions and patterns for the $^3\Sigma^-$ and $^1\Delta$ electronic states. The spin-vibronic energy levels were computed for $\mathcal{E}_1=1.5\omega$, $\mathcal{E}_2=1.6\omega$, and $\lambda/\omega=0$. Only those spin-vibronic energy levels that are associated with the $\nu=0$ and 1 harmonic-oscillator energy levels are included in this figure. The spin-vibronic energy levels have been organized in two distinct groups, each one of which is linked to the $^3\Sigma^-$ and $^1\Delta$ electronic states. These two groups of energy levels are differentiated by distinct indentations of their corresponding $\nu=0$ and 1 harmonic-oscillator labels. The far left-hand column presents the results of energy-level calculations for the unperturbed harmonic-oscillator case [column (a)]. The energy levels contained in columns (b)–(d) were calculated in the presence of pure SO coupling, representing the incremental addition of the g ($g/\omega=2.0$), d' and d ($d'/\omega=d/\omega=0.6$), and b ($b/\omega=0.04$) SO coupling parameters, respectively.

The parameter g lifts the threefold degeneracy of the ($^3\Sigma^-$, $v=0$) energy levels of $^3\Sigma^-$ vibronic symmetry into a twofold degenerate level ($^3\Sigma^-_1$) and a nondegenerate energy level ($^3\Sigma^-_{0^+}$) [see Fig. 6(b)]. The sixfold vibronic degeneracy of the ($^3\Sigma^-$, $v=1$) energy level of $^3\Pi$ vibronic symmetry is

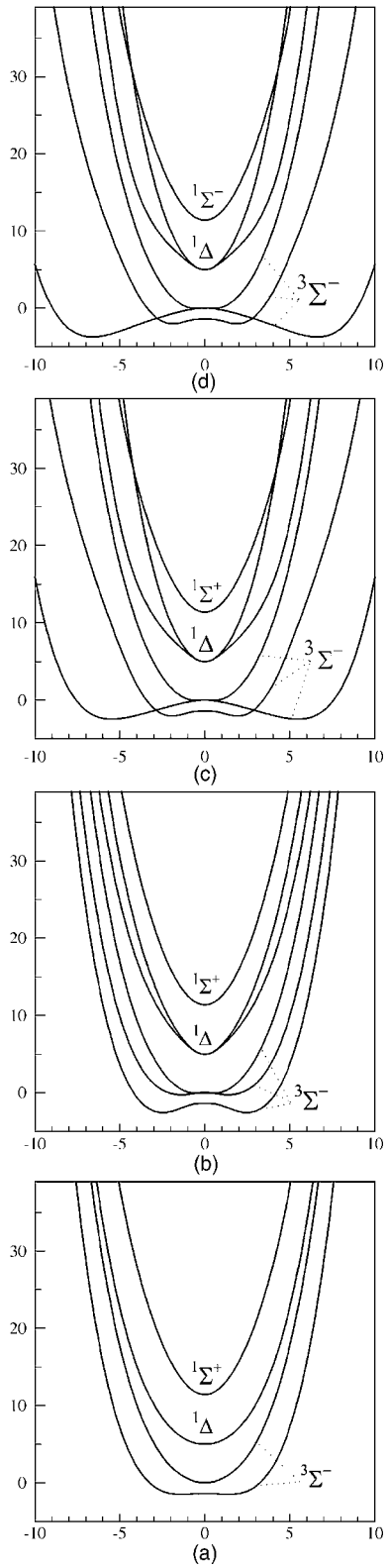

FIG. 5. Potential energy as a function of the bending coordinate for selected cases of Renner-Teller, $^1\Sigma^+-{}^1\Delta$ electrostatic, and SO-induced vibronic couplings in Σ and Δ electronic states of quasilinear triatomic molecules with a half-filled π shell. The ordinate scale is in units of ω, while the abscissa represents the dimensionless bending normal coordinate ρ. The curves shown here have been constructed for $\mathcal{E}_1=\mathcal{E}_2=5\omega$ and $\lambda/\omega=0.2$. The energy $E_{^3\Sigma^-}$ is defined as 0 for $\rho=0$. (a) $(g/\omega=4;\ d'/\omega=2;\ \lambda/\omega=0.2;\ a/\omega=0;\ c/\omega=0;\ d/\omega=0;\ b/\omega=0)$, (b) $(g/\omega=4;\ d'/\omega=2;\ d/\omega=2;\ \lambda/\omega=0.2;\ a/\omega=0;\ c/\omega=0;\ b/\omega=0)$, (c) $(g/\omega=4;\ d'/\omega=2;\ d/\omega=2;\ b/\omega=0.1;\ \lambda/\omega=0.2;\ a/\omega=0;\ c/\omega=0)$, and (d) $(a/\omega=0.002;\ c/\omega=0.04;\ g/\omega=4;\ d'/\omega=2;\ d/\omega=2;\ b/\omega=0.1;\ \lambda/\omega=0.2)$.

also lifted, producing a fourfold degenerate level ($^3\Pi_{0^\pm}+{}^3\Pi_2$) and a twofold degenerate level ($^3\Pi_1$). The vibronic degeneracy of the ($^1\Delta$, $v=1$) energy level of $^1\Pi+{}^1\Phi$ vibronic symmetry is maintained in column (b). Note that the ($^3\Sigma^-$, $v=0,1$) spin-vibronic energy levels $^3\Sigma_1^-$ and $^3\Pi_1$ are tuned into accidental quasiresonance in column (b) of Fig. 6. The inclusion of the d' and d linear coupling effects in column (c) lifts the aforementioned degeneracies and quasidegeneracy of column (b) [see column (c)]. The ($^1\Delta$, $v=1$) energy levels $^1\Pi_1$ and $^1\Phi_3$ are tuned into accidental quasidegeneracy in column (d). The value of the cubic coupling parameter b which is included in the energy-level calculation of column (d) is too small to cause significant changes of the energy-level pattern of column (c). The effects of SO vibronic coupling would be more pronounced if the $^1\Delta$ PE function had a minimum at $\rho\neq 0$, as it happens in CH_2, CHX, CX_2, SiH_2, GeH_2, etc. Then the lowest $^1\Delta$ and $^3\Sigma^-$ vibronic levels would be quasidegenerate.

IV. CONCLUSIONS

The combined effects of Renner-Teller, $^1\Sigma^+-{}^1\Delta$, as well as SO-induced vibronic coupling interactions on the PESs of the $^3\Sigma^-$, $^1\Delta$, and $^1\Sigma^+$ states arising from a half-filled π orbital of a linear triatomic molecule have been described, employing the microscopic (Breit-Pauli) expression of the SO operator. The microscopic theory involves six SO-coupled electronic wave functions with spin-orbital angular momentum projections $\Omega=\pm 2,\ \pm 1,\ 0_\pm$. The spin-vibronic Hamiltonian matrix has been constructed in the diabatic representation, considering terms up to fourth order in the bending displacement. The symmetry properties of the SO-induced as well as electrostatic vibronic coupling effects have been described in detail. We have provided the first systematic and complete analysis of the SO vibronic coupling effects in the manifold of electronic states which arise from a half-filled π orbital in a quasilinear molecule. The Taylor expansion of the vibronic matrix and the numerical calculation of the vibronic energy levels can straightforwardly be extended to higher orders if this should be necessary. The present analysis provides the foundation for a comprehensive analysis and computational prediction of the vibronic spectra of CH_2 as well as of heavier linear triatomic halogenated carbenes of the R_1CR_2 type, which are subject to increasing SO interactions, such as CHX with X=F, Cl, Br, I, their deuterated analogs, CX_2, or various molecular species such as SiH_2, GeH_2, etc.

ACKNOWLEDGMENTS

The authors thankfully acknowledge financial support by the Deutsche Forschungsgemeinschaft via a research grant as well as a visitor grant for L. V. P. This work has also been supported by the Fonds der Chemischen Industrie.

APPENDIX A: DERIVATION OF THE ($^3\Sigma^-$, $^1\Delta$, $^1\Sigma^+$) SO VIBRONIC COUPLING HAMILTONIAN

Consider the matrix elements of the electronic Hamiltonian $\hat{\mathcal{H}}_{es}+\hat{\mathcal{H}}_{SO}$ with the electronic basis functions defined in Eqs. (14)–(19). We expand $\hat{\mathcal{H}}_{es}+\hat{\mathcal{H}}_{SO}$ in powers of the

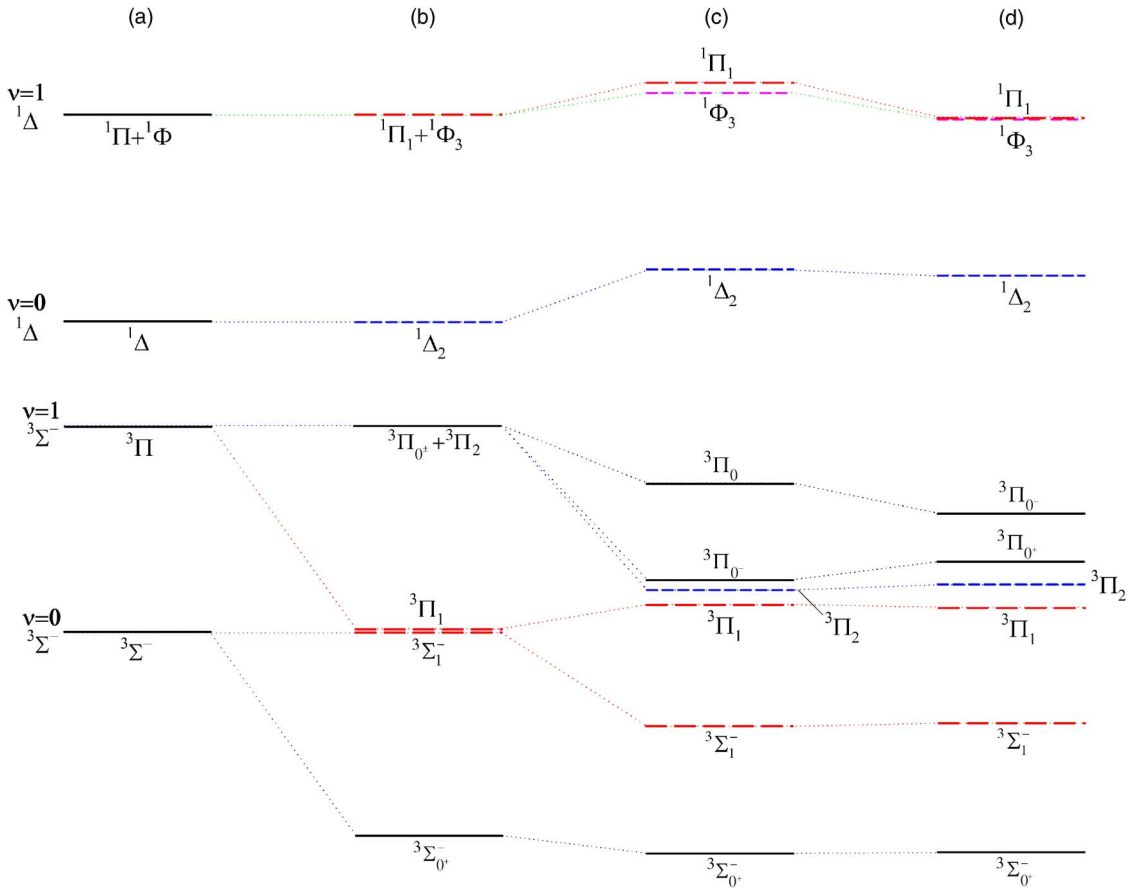

FIG. 6. (Color online) Energy-level correlation diagram of the spin-vibronic energy levels of the $^3\Sigma^-$ and $^1\Delta$ electronic states of a Renner-Teller active mode of π symmetry, calculated for selected cases of SO-induced vibronic coupling for the following parameter values: (a) ($a/\omega=0$; $c/\omega=0$; $\lambda/\omega=0$; $g/\omega=0$; $d'/\omega=0$; $d/\omega=0$; $b/\omega=0$), (b) ($a/\omega=0$; $c/\omega=0$; $\lambda/\omega=0$; $g/\omega=2.0$; $d'/\omega=0$; $d/\omega=0$; $b/\omega=0$), (c) ($a/\omega=0$; $c/\omega=0$; $\lambda/\omega=0$; $g/\omega=2.0$; $d'/\omega=0.6$; $d/\omega=0.6$; $b/\omega=0$), and (d) ($a/\omega=0$; $c/\omega=0$; $\lambda/\omega=0$; $g/\omega=2.0$; $d'/\omega=0.6$; $d/\omega=0.6$; $b/\omega=0.04$). The calculation of the energy levels assumes that $\mathcal{E}_1=1.5\omega$ and $\mathcal{E}_2=1.6\omega$. Only the spin-vibronic energy levels arising from the $\nu=0$ and 1 harmonic-oscillator levels of the $^3\Sigma^-$ and $^1\Delta$ electronic states are presented in the figure. The solid, long-dash dotted, short-dash dotted, and short-short dotted lines represent energy levels with $\mu=0$, 1, 2, and 3, respectively.

bending normal mode $Q_\pm=\rho e^{\pm i\phi}$. The requirement that the Hamiltonian must be totally symmetric with respect to the angular-momentum operator $\hat{\mathcal{J}}_z'$ leads to the following structure of the Hamiltonian matrix:

$$\mathcal{H}_{\mathrm{el}}=\begin{array}{c|cccccc} & \psi_{+2}^{+2} & \psi_{+1}^{0} & \psi_{0}^{0} & \phi_{0}^{0} & \psi_{-1}^{0} & \psi_{-2}^{-2} \\ \hline \psi_{+2}^{+2} & E_{^1\Delta} & d_1\rho e^{i\phi} & h\rho^2 e^{2i\phi} & c\rho^2 e^{2i\phi} & b\rho^3 e^{3i\phi} & a\rho^4 e^{4i\phi} \\ \psi_{+1}^{0} & d_1^\star\rho e^{-i\phi} & E_{^3\Sigma^-} & d_2\rho e^{i\phi} & d_3\rho e^{i\phi} & k\rho^2 e^{2i\phi} & b'\rho^3 e^{3i\phi} \\ \psi_{0}^{0} & h^\star\rho^2 e^{-2i\phi} & d_2^\star\rho e^{-i\phi} & E_{^3\Sigma^-} & g & d_3'\rho e^{i\phi} & h'\rho^2 e^{2i\phi} \\ \phi_{0}^{0} & c^\star\rho^2 e^{-2i\phi} & d_3^\star\rho e^{-i\phi} & g^\star & E_{^1\Sigma^+} & d_2'\rho e^{i\phi} & c\rho^2 e^{2i\phi} \\ \psi_{-1}^{0} & b^\star\rho^3 e^{-3i\phi} & k^\star\rho^2 e^{-2i\phi} & d_3'^\star\rho e^{-i\phi} & d_2'^\star\rho e^{-i\phi} & E_{^3\Sigma^-} & d_1'\rho e^{i\phi} \\ \psi_{-2}^{-2} & a^\star\rho^4 e^{-4i\phi} & b'^\star\rho^3 e^{-3i\phi} & h'^\star\rho^2 e^{-2i\phi} & c^\star\rho^2 e^{-2i\phi} & d_1'^\star\rho e^{-i\phi} & E_{^1\Delta} \end{array}. \quad \text{(A1)}$$

The diagonal elements of the matrix (A1) and the elements $c\rho^2e^{2i\phi}$ and $a\rho^4e^{4i\phi}$ arise from the electrostatic Hamiltonian $\hat{\mathcal{H}}_{\mathrm{es}}$. The parameter c represents the vibronic coupling of the $^1\Delta$ state and the $^1\Sigma^+$ state in second order of the bending displacement. The parameter a represents the fourth-order Renner-Teller coupling within the $^1\Delta$ state. All other matrix elements of Eq. (A1) arise from the SO operator.

We include only the lowest-order nonvanishing contribution for each matrix element and ignore SO corrections to matrix elements of the electrostatic Hamiltonian. It can be shown by explicit calculation of matrix elements with the basis functions (14)–(19) that the coupling parameters $a,b,c,d,\ldots$ are real. The diagonal matrix elements have the expansion

$$E_{^1\Delta} = E^{(0)}_{^1\Delta} + \tfrac{1}{2}\omega\rho^2 + \tfrac{1}{24}\lambda\rho^4 + \cdots, \tag{A2}$$

$$E_{^3\Sigma^-} = E^{(0)}_{^3\Sigma^-} + \tfrac{1}{2}\omega\rho^2 + \tfrac{1}{24}\lambda\rho^4 + \cdots, \tag{A3}$$

$$E_{^1\Sigma^+} = E^{(0)}_{^1\Sigma^+} + \tfrac{1}{2}\omega\rho^2 + \tfrac{1}{24}\lambda\rho^4 + \cdots, \tag{A4}$$

where we have assumed, for simplicity, that the bending vibrational frequency ω and the anharmonicity parameter λ are the same in the three electronic states arising from the π^2 configuration.

Requiring the vanishing of the commutator of the Hamiltonian matrix (A1) with the time-reversal operator (24), we obtain the relations $b'=-b$, $d_1'=-d_1$, $d_2'=-d_3$, $d_3'=-d_2$, $h'=h$, and thus,

$$\mathcal{H}_{\mathrm{el}} = \left(\tfrac{1}{2}\omega\rho^2 + \tfrac{1}{24}\lambda\rho^4\right)1 + \begin{bmatrix} E^{(0)}_{^1\Delta} & d_1\rho e^{i\phi} & h\rho^2 e^{2i\phi} & c\rho^2 e^{2i\phi} & b\rho^3 e^{3i\phi} & a\rho^4 e^{4i\phi} \\ d_1\rho e^{-i\phi} & E^{(0)}_{^3\Sigma^-} & d_2\rho e^{i\phi} & d_3\rho e^{i\phi} & k\rho^2 e^{2i\phi} & -b\rho^3 e^{3i\phi} \\ h\rho^2 e^{-2i\phi} & d_2\rho e^{-i\phi} & E^{(0)}_{^3\Sigma^-} & g & -d_2\rho e^{i\phi} & h\rho^2 e^{2i\phi} \\ c\rho^2 e^{-2i\phi} & d_3\rho e^{-i\phi} & g & E^{(0)}_{^1\Sigma^+} & -d_3\rho e^{i\phi} & c\rho^2 e^{2i\phi} \\ b\rho^3 e^{-3i\phi} & k\rho^2 e^{-2i\phi} & -d_2\rho e^{-i\phi} & -d_3\rho e^{-i\phi} & E^{(0)}_{^3\Sigma^-} & -d_1\rho e^{i\phi} \\ a\rho^4 e^{-4i\phi} & -b\rho^3 e^{-3i\phi} & h\rho^2 e^{-2i\phi} & c\rho^2 e^{-2i\phi} & -d_1\rho e^{-i\phi} & E^{(0)}_{^1\Delta} \end{bmatrix}. \tag{A5}$$

The matrix (A5) can be further simplified by the explicit calculation of matrix elements of the SO operator of Eqs. (4)–(6) with the electronic basis functions (14)–(19). It is convenient to write $\hat{\mathcal{H}}_{\mathrm{SO}}$ as an expansion in the bending amplitude ρ,

$$\hat{\mathcal{H}}_{\mathrm{SO}} = \hat{\mathcal{H}}^{(0)}_{\mathrm{SO}} + \hat{\mathcal{H}}^{(1)}_{\mathrm{SO}} + \hat{\mathcal{H}}^{(2)}_{\mathrm{SO}} + \cdots. \tag{A6}$$

The leading term can be written as

$$\hat{\mathcal{H}}^{(0)}_{\mathrm{SO}} = \kappa(\mathbf{S}_1 \cdot \boldsymbol{\mathcal{K}}_1 + \mathbf{S}_2 \cdot \boldsymbol{\mathcal{K}}_2), \tag{A7}$$

with

$$\kappa = \tfrac{1}{2} i g \beta_e^2,$$

$$\boldsymbol{\mathcal{K}}_1 = -\sum_n \frac{Q_n}{r_{1n}^3}(\mathbf{r}_{1n} \times \boldsymbol{\nabla}_1) + \frac{1}{r_{12}^3}[\mathbf{r}_{12} \times (\boldsymbol{\nabla}_1 - 2\boldsymbol{\nabla}_2)], \tag{A8}$$

$$\boldsymbol{\mathcal{K}}_2 = -\sum_n \frac{Q_n}{r_{2n}^3}(\mathbf{r}_{2n} \times \boldsymbol{\nabla}_2) + \frac{1}{r_{21}^3}[\mathbf{r}_{21} \times (\boldsymbol{\nabla}_2 - 2\boldsymbol{\nabla}_1)].$$

The higher-order terms can analogously be written as

$$\hat{\mathcal{H}}^{(1)}_{\mathrm{SO}} = \kappa(\mathbf{S}_1 \cdot \boldsymbol{\mathcal{L}}_1 + \mathbf{S}_2 \cdot \boldsymbol{\mathcal{L}}_2),$$

$$\hat{\mathcal{H}}^{(2)}_{\mathrm{SO}} = \kappa(\mathbf{S}_1 \cdot \boldsymbol{\mathcal{Q}}_1 + \mathbf{S}_2 \cdot \boldsymbol{\mathcal{Q}}_2), \tag{A9}$$

$$\hat{\mathcal{H}}^{(3)}_{\mathrm{SO}} = \kappa(\mathbf{S}_1 \cdot \boldsymbol{\mathcal{R}}_1 + \mathbf{S}_2 \cdot \boldsymbol{\mathcal{R}}_2).$$

The operators $\boldsymbol{\mathcal{L}}_k$, $\boldsymbol{\mathcal{Q}}_k$, and $\boldsymbol{\mathcal{R}}_k$, $k=1,2$, are differential operators in electronic coordinate space and can be obtained from the $\boldsymbol{\mathcal{K}}_k$ by somewhat lengthy calculations.

It is obvious that the parameter k in Eq. (A5) vanishes by spin integration, since the basis functions differ in two spin orbitals, while $\hat{\mathcal{H}}_{\mathrm{SO}}$ is a single-particle operator in spin space. It is straightforward to show that the matrix element

$$h\rho^2 e^{2i\phi} = \langle \psi^0_0 | \hat{\mathcal{H}}^{(2)}_{\mathrm{SO}} | \psi^{-2}_{-2} \rangle \tag{A10}$$

vanishes by spin integration. For the matrix element

$$\langle \psi^0_{+1} | \hat{\mathcal{H}}^{(1)}_{\mathrm{SO}} | \psi^0_0 \rangle = d_2\rho e^{i\phi},$$

it can be shown that

$$\langle \psi^0_0 | \hat{\mathcal{H}}^{(1)}_{\mathrm{SO}} | \psi^0_{+1} \rangle^\star = -\langle \psi^0_{+1} | \hat{\mathcal{H}}^{(1)}_{\mathrm{SO}} | \psi^0_0 \rangle.$$

Since $\hat{\mathcal{H}}_{\mathrm{el}}$ must be Hermitian, this implies $d_2=0$. With the simplified notation $d_1=d$, $d_3=d'$, we have the Hamiltonian of Eq. (25).

APPENDIX B: VIBRATIONAL MATRIX ELEMENTS OF THE VIBRONIC MOLECULAR HAMILTONIAN $\hat{\mathcal{H}}$ IN THE BASIS SET OF THE TWO-DIMENSIONAL ISOTROPIC HARMONIC OSCILLATOR

$$\langle n,l|d^{(\prime)}\rho e^{\mp i\phi}|n+1,l\pm 1\rangle = d^{(\prime)}\left[\tfrac{1}{2}(n\pm l+2)\right]^{1/2},$$

$$\langle n,l|d^{(\prime)}\rho e^{\mp i\phi}|n-1,l\pm 1\rangle = d^{(\prime)}\left[\tfrac{1}{2}(n\mp l)\right]^{1/2},$$

$$\left\langle n,l\left|\hat{\mathcal{T}}_N+\tfrac{1}{2}\omega\rho^2\right|n,l\right\rangle = \hbar\omega(n+1),$$

$$\langle n,l|c\rho^2 e^{\mp 2i\phi}|n+2,l\pm 2\rangle = c\left[\left(\tfrac{1}{2}\right)^2(n\pm l+2)\times(n\pm l+4)\right]^{1/2},$$

$$\langle n,l|c\rho^2 e^{\mp 2i\phi}|n,l\pm 2\rangle = 2c\left[\left(\tfrac{1}{2}\right)^2(n\mp l)(n\pm l+2)\right]^{1/2},$$

$$\langle n,l|c\rho^2 e^{\mp 2i\phi}|n-2,l\pm 2\rangle = c\left[\left(\tfrac{1}{2}\right)^2(n\mp l)(n\mp l-2)\right]^{1/2},$$

$$\langle n,l|b\rho^3 e^{\mp 3i\phi}|n+3,l\pm 3\rangle = b\left[\left(\tfrac{1}{2}\right)^3(n\pm l+2)(n\pm l+4)\times(n\pm l+6)\right]^{1/2},$$

$$\langle n,l|b\rho^3 e^{\mp 3i\phi}|n+1,l\pm 3\rangle = 3b\left[\left(\tfrac{1}{2}\right)^3(n\pm l+2)\times(n\pm l+4)(n\mp l)\right]^{1/2},$$

$$\langle n,l|b\rho^3 e^{\mp 3i\phi}|n-1,l\pm 3\rangle = 3b\left[\left(\tfrac{1}{2}\right)^3(n\mp l)(n-l\mp 2)\times(n+l\pm 2)\right]^{1/2},$$

$$\langle n,l|b\rho^3 e^{\mp 3i\phi}|n-3,l\pm 3\rangle = b\left[\left(\tfrac{1}{2}\right)^3(n\mp l)(n\mp l-2)\times(n\mp l-4)\right]^{1/2},$$

$$\langle n,l|a\rho^4 e^{\mp 4i\phi}|n+4,l\pm 4\rangle = a\left[\left(\tfrac{1}{2}\right)^4(n\pm l+2)(n\pm l+4)\times(n\pm l+6)(n\pm l+8)\right]^{1/2},$$

$$\langle n,l|a\rho^4 e^{\mp 4i\phi}|n+2,l\pm 4\rangle = 4a\left[\left(\tfrac{1}{2}\right)^4(n\mp l)(n\pm l+2)\times(n\pm l+4)(n\pm l+6)\right]^{1/2},$$

$$\langle n,l|\frac{1}{4!}\lambda\rho^4|n,l\rangle = \lambda\left(\tfrac{1}{2}\right)^4(n-l+2)(n-l+4),$$

$$\langle n,l|a\rho^4 e^{\mp 4i\phi}|n,l\pm 4\rangle = 6a\left[\left(\tfrac{1}{2}\right)^4(n\mp l)(n\mp l-2)\times(n\pm l+2)(n\pm l+4)\right]^{1/2},$$

$$\langle n,l|a\rho^4 e^{\mp 4i\phi}|n-2,l\pm 4\rangle = 4a\left[\left(\tfrac{1}{2}\right)^4(n\mp l)(n\mp l-2)\times(n\mp l-4)(n\pm l+2)\right]^{1/2},$$

$$\langle n,l|a\rho^4 e^{\mp 4i\phi}|n-4,l\pm 4\rangle = a\left[\left(\tfrac{1}{2}\right)^4(n\mp l)(n\mp l-2)\times(n\mp l-4)(n\mp l-6)\right]^{1/2}.$$

[1] L. V. Poluyanov and W. Domcke, Chem. Phys. **301**, 111 (2004).
[2] S. Mishra, V. Vallet, L. V. Poluyanov, and W. Domcke, J. Chem. Phys. **123**, 124104 (2005).
[3] S. Mishra, L. V. Poluyanov, and W. Domcke, J. Chem. Phys. **126**, 134312 (2007).
[4] U. E. Weirsum and L. W. Jenneskens, *Gas Phase Reactions in Organic Synthesis*, edited by V. Vallée (Gordon and Breach, Australia, 1997).
[5] A. M. Dean and J. W. Bozzelli, *Gas-phase Combustion Chemistry*, edited by W. C. Gardiner, Jr. (Springer, New York, 2000), Chap. 2.
[6] R. P. Wayne, *Chemistry of Atmospheres* (Oxford University Press, Oxford, 1991), Chap. 8, and references therein.
[7] G. Winnewisser and E. Herbst, Rep. Prog. Phys. **56**, 1209 (1993).
[8] E. Herbst, Angew. Chem., Int. Ed. Engl. **29**, 595 (1990).
[9] *Carbenes*, Reactive Intermediates in Organic Chemistry Series, edited by R. A. Moss and M. Jones, Jr. (Wiley-Interscience, New York, 1973), Vol. 1; (Wiley-Interscience, New York, 1975), Vol. 2.
[10] W. Kirmse, *Carbene Chemistry* (Academic, New York, 1971).
[11] J. C. Sciano, *Handbook of Organic Photochemistry* (CRC, Boca Raton, FL, 1989), Vol. 2, Chap. 9.
[12] F. A. Carey and R. J. Sundberg, in *Advanced Organic Chemistry, Part 3* (Plenum, New York, 1990).
[13] K. Sendt, G. B. Bacskay, and J. C. Mackie, J. Phys. Chem. A **104**, 1861 (2000), and references therein.
[14] K. Kobayashi, L. D. Pride, and T. J. Sears, J. Chem. Phys. **104**, 10119 (2000).
[15] Y. Kim, A. V. Kommisarov, G. E. Hall, and T. J. Sears, J. Chem. Phys. **123**, 024306 (2005).
[16] A. V. Kommisarov, A. Lin, T. J. Sears, and G. E. Hall, J. Chem. Phys. **125**, 084308 (2006).
[17] S. K. Shih, S. D. Peyerimhoff, R. J. Buenker, and M. Peric, Chem. Phys. Lett. **55**, 206 (1978).
[18] P. Saxe, H. F. Schaefer, and N. C. Handy, J. Phys. Chem. **85**, 745 (1981).
[19] P. J. Reynolds, M. Dupuis, and W. A. Lester, J. Chem. Phys. **82**, 1983 (1985).
[20] H.-G. Yu, J. T. Muckerman, and T. J. Sears, J. Chem. Phys. **116**, 1435 (2002), and references therein.
[21] C. Tao, C. Mukarakate, and S. A. Reid, J. Chem. Phys. **124**, 224314 (2006), and references therein.
[22] G. Duxbury and C. Jungen, Mol. Phys. **63**, 981 (1988).
[23] A. Alijah and G. Duxbury, Mol. Phys. **70**, 605 (1990).
[24] G. Duxbury, B. D. McDonald, M. van Gogh, A. Alijah, C. Jungen, and H. Palivan, J. Chem. Phys. **108**, 2336 (1998).
[25] J.-P. Gu, G. Hirsch, R. J. Buenker, M. Brumm, G. Osmann, P. R. Bunker, and P. Jensen, J. Mol. Struct. **517**, 247 (2000).
[26] S. Mishra, W. Domcke, and L. V. Poluyanov, Chem. Phys. **327**, 457 (2006).
[27] S. Mishra, V. Vallet, L. V. Poluyanov, and W. Domcke, J. Chem. Phys. **125**, 164327 (2006).
[28] H. Köppel, W. Domcke, and L. S. Cederbaum, J. Chem. Phys. **74**, 2945 (1981).
[29] H. Köppel, W. Domcke, and L. S. Cederbaum, Adv. Chem. Phys. **57**, 59 (1984).
[30] H. Lefebvre–Brion and R. W. Field, *The Spectra and Dynamics of Diatomic Molecules* (Elsevier, New York, 2004).
[31] E. Wigner, *Group Theory* (Academic Press, New York, 1959).
[32] L. D. Landau and E. M. Lifshitz, *Quantum Mechanics* (Nauka, Moscow, 1974).
[33] W. Lichten, Phys. Rev. **164**, 131 (1967).
[34] F. T. Smith, Phys. Rev. **179**, 111 (1969).
[35] T. Pacher, L. S. Cederbaum, and H. Köppel, Adv. Chem. Phys. **84**, 293 (1993).
[36] J. T. Hougen, J. Chem. Phys. **36**, 1874 (1962).
[37] G. Herzberg, *Electronic Spectra and Electronic Structure of Polyatomic Molecules, Molecular Spectra and Molecular Structure* (Van Nostrand, New York, 1966), Vol. 3.
[38] L. Schiff, *Quantum Mechanics*, 3rd ed. (McGraw-Hill, New York, 1968).
[39] J. A. Pople and H. C. Longuet–Higgins, Mol. Phys. **1**, 372 (1958).
[40] J. M. Brown and F. Jørgensen, Mol. Phys. **47**, 1065 (1982).